An Integrated Battery Charger for EVs Based on an Asymmetrical Six-Phase Machine

I. Subotic, E. Levi, M. Jones
Liverpool John Moores University, Liverpool L3 3AF, U.K.
i.subotic@2011.ljmu.ac.uk, e.levi@ljmu.ac.uk, m.jones2@ljmu.ac.uk

D. Graovac
Infineon, D-85579 Neubiberg, Germany
dusan.graovac@infineon.com

***Abstract*–The paper considers a novel battery charger topology for electrical vehicles (EVs) that utilises an asymmetrical six-phase propulsion machine. A six-phase inverter and the machine are fully integrated into the charging process. The proposed integrated battery charger has the advantages of unity power factor operation and zero average torque production in the machine during the charging mode. The operating principles are based on the additional degrees of freedom that exist in multiphase machines and it is shown that asymmetrical six-phase machines can be conveniently utilised to achieve charging through the machine's stator winding while developing zero electromagnetic torque. Detailed theoretical analysis is reported for the asymmetrical six-phase charging system. A mathematical model of the six-phase voltage source rectifier (VSR) is given, control in the charging mode is discussed, and the theoretical considerations are validated by simulations.**

I. Introduction

Non-integrated chargers are at present standard in automotive industry. However, if the existing propulsion mode related power electronics components are integrated into the charging process, benefits could be remarkable. Cost, which is very high [1], could be significantly reduced. Next, by avoiding installation of additional elements space could be saved and the weight decreased. An integrated charger was developed for the first time in 1985 [2], and many various integrated solutions have been reported since [3].

The majority of EVs at present use a machine of either induction or permanent magnet synchronous type for propulsion [4]. Currently, there are only five integrated on-board solutions [5-9] that allow fast (three-phase) charging incorporating these types of machines. In [5], during the charging mode, motor three-phase stator windings are in an open-end winding configuration, with one end connected to the inverter, while the other three winding terminals at the other side are connected to a three-phase grid. Development of the rotating field occurs during the charging mode, so the motor must be mechanically locked during the charging process, which is a severe drawback. In [6], in order to provide a galvanic isolation, an induction machine is used like a transformer in the battery charging mode. However, this solution increases the cost of the drive system since it requires a wound rotor, so that the isolation advantage is completely overshadowed. Another isolated solution is presented in [7]. It avoids the additional cost of a wound rotor by having a stator with two sets of three-phase windings, which are shifted spatially by 30 degrees (split-phase or asymmetrical six-phase configuration). In the traction mode each pair of phases of the two three-phase windings that has spatial shift of 30 degrees is connected in series to constitute a single three-phase winding set. For the charging mode the system requires reconfiguration. The first set of three-phase windings is connected to the inverter on one side, and into the star on the other side, while the second set is connected into delta on one side, and to the grid at the other side. In contrast to the previous two, this solution has an exploitation potential.

A completely different charger topology is proposed in [8]. The solution uses mid-points of each of the three windings of a three-phase machine to connect them to a three-phase ac grid during charging (three-phase machine with accessible mid-points is in essence an equivalent of a symmetrical six-phase machine). Compared to the three previous configurations, this one has some distinct advantages: there is no torque production in the machine during charging mode; moreover, no hardware reconfiguration between propulsion and charging mode of operation is required.

A configuration with the same advantages as in [8] but based on a nine-phase machine is suggested in [9]. Terminals of a three-phase grid are directly connected to three isolated neutral points of a nine-phase machine, and, by simultaneous control of inverter legs attached to the same machine's three-phase winding set, torque-free operation is ensured.

This brief survey of the state-of-the-art shows that only the solutions based on, in essence, multiphase machines have the advantage of no average torque production during the charging operation.

Multiphase drives ($n > 3$) are mainly aimed at high power/ high current applications. Their two main advantages over three-phase systems are reduced current (power) rating of the semiconductor switches and excellent fault-tolerant operation features [10]. Multiphase machines are characterised with existence of additional degrees of freedom with regard to the control. This brings in an added advantage over their three-phase counterparts in applications related to the integrated charging of EVs, since these additional degrees of freedom can be used for battery charging without any average torque production, as shown further in this paper, which for the first time considers asymmetrical six-phase supply as a fast charging option for EVs.

Developed novel six-phase integrated charging solution is characterised with a unity power factor operation, while the machine is kept naturally at standstill during the charging process. The inverter and the machine are fully integrated into the charging process. The configuration employs phase transposition rules [11] in order to ensure that the motor does not develop average torque during charging; hence the machine naturally remains at standstill and its stator winding

Pre-print. Final version of this paper appears in IEEE Xplore Digital Library (http://ieeexplore.ieee.org/Xplore/guesthome.jsp).

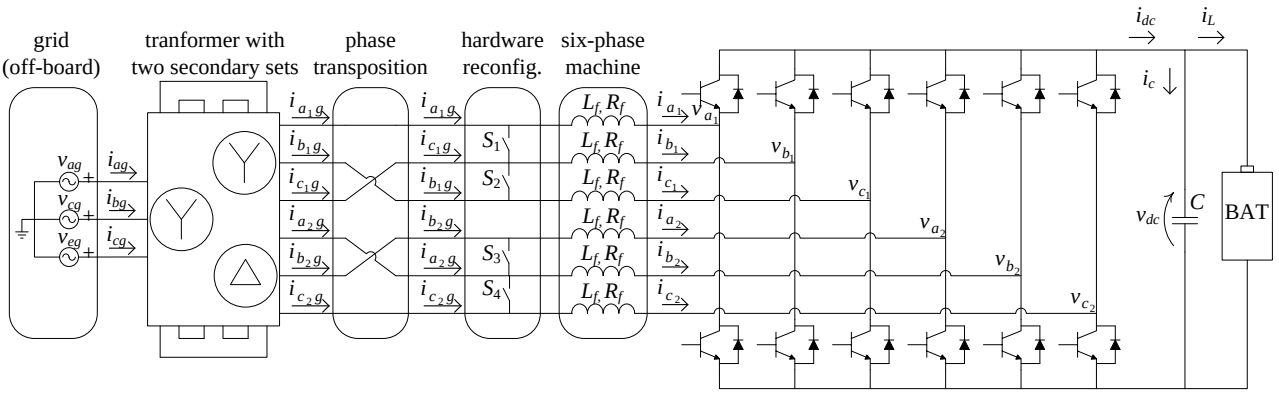

Fig. 1. Topology of the asymmetrical six-phase integrated battery charging system.

leakage inductances are utilised for filtering during the charging process.

The paper is organized as follows. In Section II theoretical analysis is provided for the asymmetrical six-phase charging system. A mathematical model of a six-phase VSR is presented in Section III. In Section IV the control algorithm for the proposed configuration is given. In Section V theoretical results are validated by simulations for both charging and vehicle-to-grid (V2G) mode. The conclusions are summarised in Section VI.

II. Operating Principles of an Asymmetrical Six-Phase Charging System

An asymmetrical six-phase machine can be used in integrated configurations that allow single-phase charging, [12]. However, single-phase systems allow only slow charging. In this Section this machine type is considered for the fast multiphase battery charging.

For charging purposes two neutral points of the machine are opened and the phases are connected to the sinusoidal asymmetrical six-phase source which is obtained from a three-phase transformer with a dual secondary winding. By connecting the two secondary windings in star and delta, respectively, required supply phase shift between two three-phase windings of 30 degrees is achieved (the voltage levels are made the same by proper selection of the turn numbers for the secondaries). However, instead of connecting the motor phases a_1 to c_2 directly to a_1 to c_2 phases of the supply, the principle of phase transposition [11] is applied to insure operation with the zero average torque. The resulting connection diagram for the charging mode is as shown in Fig. 1. It can be seen that machine phases a_1 and c_2 are connected to grid phases a_1g and c_2g. Yet, machine phases b_1, c_1, a_2 and b_2 are now connected to grid phases c_1g, b_1g, b_2g and a_2g respectively, all according to the phase transposition rules [11]. Parameters R_f and L_f in Fig. 1 in essence represent stator leakage impedance of the six-phase machine.

The decoupling (Clarke's) transformation matrix for asymmetrical six-phase machines is well-known and is available in, for example, [10]. For theoretical considerations, it is advantageous to combine pairs of rows in 2D space vectors, which can be formulated as (f stands for any variable that is being transformed, e.g. current, voltage, etc.):

$$\begin{aligned}\underline{f}_{\alpha\beta} &= \sqrt{2/6}\left(f_{a_1} + \underline{a}^4 f_{b_1} + \underline{a}^8 f_{c_1} + \underline{a} f_{a_2} + \underline{a}^5 f_{b_2} + \underline{a}^9 f_{c_2}\right)\\ \underline{f}_{xy} &= \sqrt{2/6}\left(f_{a_1} + \underline{a}^8 f_{b_1} + \underline{a}^{16} f_{c_1} + \underline{a}^5 f_{a_2} + \underline{a} f_{b_2} + \underline{a}^9 f_{c_2}\right)\end{aligned} \quad (1)$$

where $\underline{a} = \exp(j\alpha) = \cos\alpha + j\sin\alpha$ and $\alpha = \pi/6$.

The grid currents can be given as

$$\begin{aligned} i_{a_1 g} &= \sqrt{2} I \cos(\omega t) \quad ; i_{b_1 g} = \sqrt{2} I \cos(\omega t - 4\pi/6)\\ i_{c_1 g} &= \sqrt{2} I \cos(\omega t - 8\pi/6); i_{a_2 g} = \sqrt{2} I \cos(\omega t - \pi/6)\\ i_{b_2 g} &= \sqrt{2} I \cos(\omega t - 5\pi/6); i_{c_2 g} = \sqrt{2} I \cos(\omega t - 9\pi/6)\end{aligned} \quad (2)$$

The relationship between machine and grid phase currents is, according to Fig. 1, given with

$$\begin{aligned} i_{a_1} &= i_{a_1 g} \quad i_{b_1} = i_{c_1 g} \quad i_{c_1} = i_{b_1 g}\\ i_{a_2} &= i_{b_2 g} \quad i_{b_2} = i_{a_2 g} \quad i_{c_2} = i_{c_2 g}\end{aligned} \quad (3)$$

By substitution of (2) and (3) into (1), the following two space vectors are obtained:

$$\underline{i}_{\alpha\beta} = 0 \quad (4)$$

$$\underline{i}_{xy} = \sqrt{6} I \exp(j\omega t) \quad (5)$$

Clearly, the flux/torque producing plane ($\alpha\beta$) is not excited and the grid currents flow through the xy plane, so that the machine stays at standstill. Zero-sequence components are both equal to zero.

III. Modeling of Six-Phase Voltage Source Rectifiers

Three-phase VSR model and its control can be regarded as well-known [13]. This however is not the case with multiphase VSRs. Mathematical model of a multiphase VSR with an even number of phases in a synchronously rotating reference frame can be given with

$$\begin{aligned}\left[v_{g(dq)}\right] = L_f \frac{d\left[i_{g(dq)}\right]}{dt} - L_f \begin{bmatrix} 0 & \omega_g & 0 & \dots & 0\\ -\omega_g & 0 & 0 & \cdots & 0\\ 0 & 0 & 0 & \cdots & 0\\ \vdots & \vdots & \vdots & \ddots & \vdots\\ 0 & 0 & 0 & \dots & 0 \end{bmatrix} \cdot \left[i_{g(dq)}\right] +\\ + R_f \left[i_{g(dq)}\right] + v_{dc} \cdot \left([I]_{n\times n} - \begin{bmatrix} [0]_{(n-2)\times(n-2)} & \begin{matrix} 0 & 0\\ \vdots & \vdots \end{matrix}\\ \begin{matrix} 0 & \dots \end{matrix} & \begin{matrix} 1 & 0\\ 0 & 0 \end{matrix} \end{bmatrix}_{n\times n} \right) \left[s_{(dq)}\right]\end{aligned} \quad (6)$$

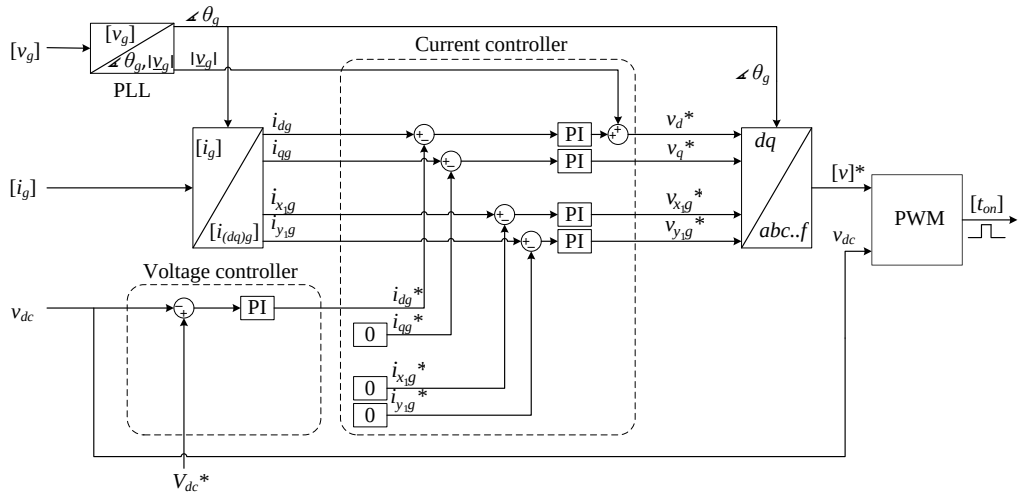

Fig. 2. Controller structure for the charging process.

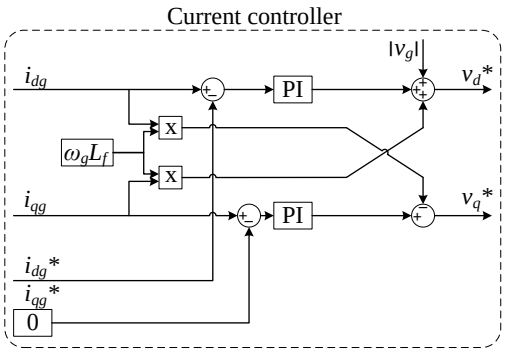

Fig. 3. Decoupling network.

$$C\frac{dv_{dc}}{dt}=[s_{(dq)}]^T\cdot[i_{g(dq)}]-i_L \quad (7)$$

where $[v_{g(dq)}]$ is the grid phase voltage matrix, $[i_{g(dq)}]$ the grid phase current matrix, and $[s_{(dq)}]$ the matrix of switching states, all in the rotating reference frame.

IV. Control of Asymmetrical Six-Phase Voltage Source Rectifiers

In the charging mode the configuration is operated according to the grid voltage oriented control (VOC) algorithm, using the control scheme presented in Fig. 2. Measurements of the grid voltages, grid currents, and dc-bus voltage are required for the closed-loop control.

The common manner of obtaining the grid voltage position is a phase-locked loop (PLL). When this information is obtained it is used to transform phase currents into the rotating reference frame that is grid voltage oriented. If the grid current has only the *d*-component the charging is with a unity power factor. Thus, the current controller aims to keep the other current components at zero, while charging the battery by the *d*-component. As can be seen from Fig. 2, multiphase rectifiers, in contrast to the three-phase systems, require more than two current controllers. The *d*-component is directly proportional to the battery charging current, thus its value is obtained by a PI voltage controller which is presented in Fig. 2.

From (6) it can be seen that there are coupling terms between the *d*- and *q*-components. Thus current control requires a decoupling network, which is for simplicity omitted in Fig. 2 and is shown separately in Fig. 3.

PWM used is of the carrier-based type, with the zero-sequence injection. However, due to the presence of two isolated (by virtue of the transformer existence) sets of three phase systems (a_1-b_1-c_1 and a_2-b_2-c_2), zero-sequence current from one set cannot flow into the other, so that it is possible to inject standard three-phase system's zero-sequence components to these sets. This increases modulation index in the linear PWM mode to the same value as in the three-phase systems.

In the propulsion mode the drive is operated according to the field oriented control (FOC), which is a well-known control method for multiphase motor drives [14].

V. Simulation Results

To verify theoretical principles of Section II and the controller structure of Section IV, simulation of the asymmetrical six-phase system is performed in Matlab/ Simulink environment. Asymmetrical six-phase grid is assumed to be already available. It has 240V voltage rms value, 50Hz frequency, and is assumed to be perfectly sinusoidal. Converter is working at 10kHz, and dead-time effect is neglected. Dc-bus capacitance is 1.5mF. Battery is represented as a simple resistor of value R_L=0.5Ω in series with an ideal voltage source *E*. The 50Hz asymmetrical six-phase induction machine has the following parameters: R_s = 12.5Ω, R_r = 6Ω, $L_{\gamma s}$ = 5.5mH, $L_{\gamma r}$ = 11mH, L_m = 590mH, three pole pairs, J = 0.1kgm^2. Both charging and vehicle-to-grid (V2G) operating modes are examined. Charging mode of operation is considered first.

A. Charging Mode of the Asymmetrical Six-Phase System

Charging mode is simulated with a value of the ideal voltage of a battery of *E*=597V. However, it is common for EVs to have a dc-dc converter between the battery and the converter so that the dc-bus voltage can be adjustable to various values. Thus the value of *E*=597V is not a necessity if

a dc-dc converter is employed (in the next subsection a different value is considered). The reference value for the dc-bus voltage is set to 600V.

In Fig. 4a grid phase voltage v_{a1g} and grid current i_{a1g} are depicted. It can be seen that the current is in essence in phase with the voltage, indicating a unity power factor operation. Relatively high ripple in the current is caused by the small leakage inductance of an existing machine. Fig. 4b shows that the grid current spectrum contains only small values of low order harmonics. Fig. 4c illustrates grid-side current *d*- and *q*-axis components. It can be seen that during the charging process the *q*-axis current component is kept at zero value, while the *d*-axis current component is kept at a constant value, which is governed by the dc-bus voltage controller. However, six-phase grid currents have additional *xy* components, and they are controlled to zero. This manner of operation allows charging with unity power factor, as can be seen from Fig. 4c, since the control is grid voltage oriented.

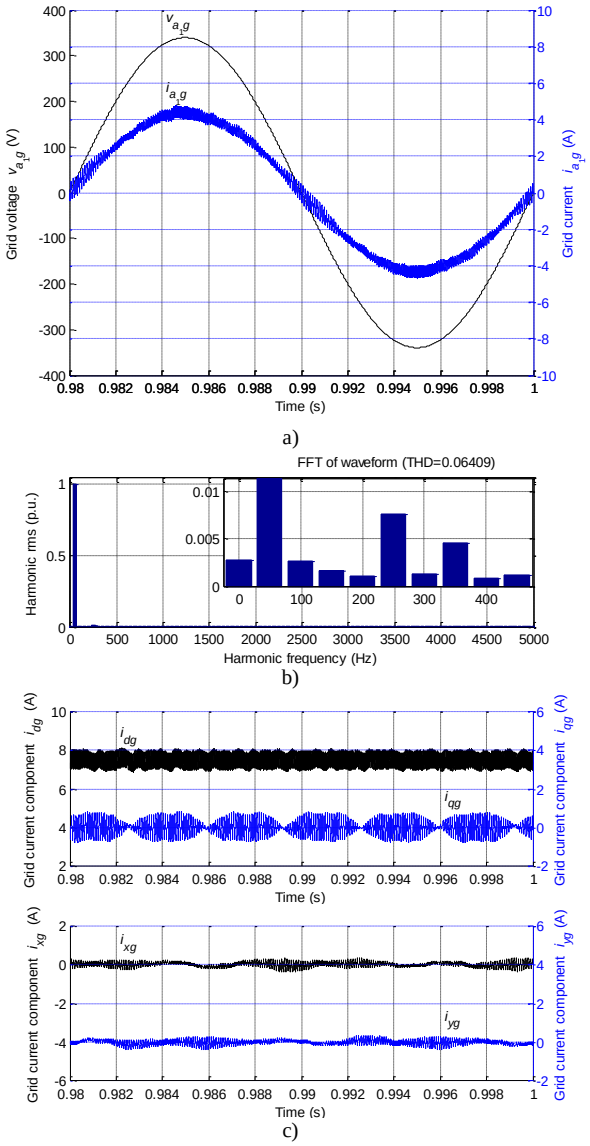

Fig. 4. Charging mode: (a) Grid phase voltage and current, (b) grid current spectrum, (c) grid current components.

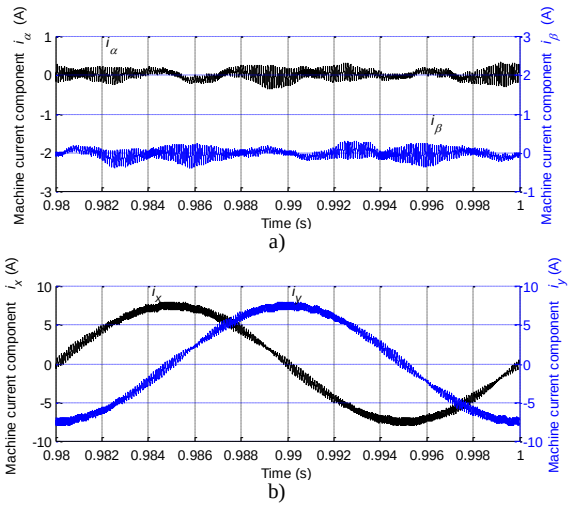

Fig. 5. Machine current componets: (a) i_α and i_β, (b) i_x and i_y.

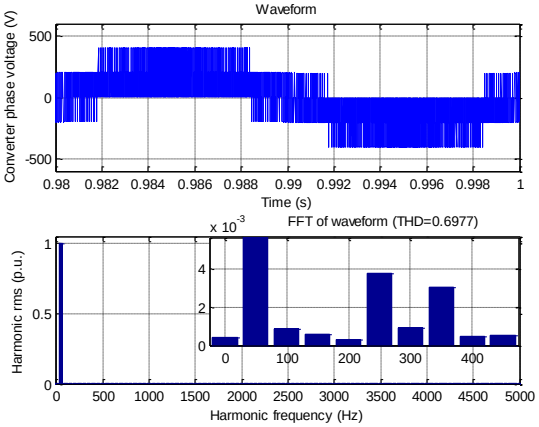

Fig. 6. Converter phase voltage and its spectrum.

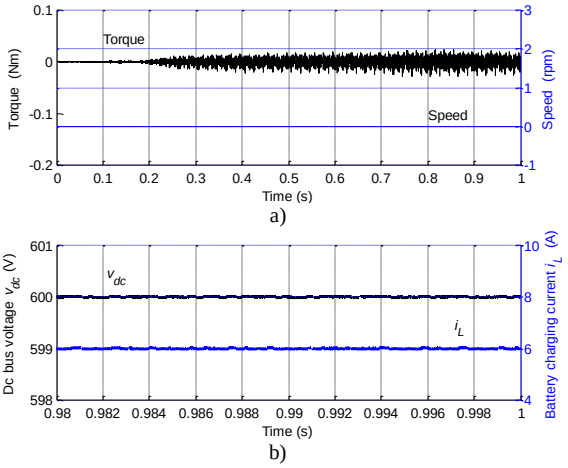

Fig. 7. (a) Machine torque and speed, (b) dc-bus voltage and charging current.

Machine phase current is the same as the grid phase current presented in Fig. 4a, but its current components are different than the grid current components, and they are presented in Fig. 5. In Fig. 5a it is shown that current components in the first plane ($\alpha\beta$) are controlled to zero, thus there will be no excitation in the first plane, and hence no torque production. In Fig. 5b current components in the second (*xy*) plane are presented, and it is obvious that this plane is responsible for

power transfer from the grid to the battery, which is in accordance with the theoretical results from (4) and (5).

Converter phase voltage and its spectrum are presented in Fig. 6. Since the dead time is neglected, low order harmonics are practically non-existent.

Machine's torque and speed are shown in Fig. 7a. The torque average value is zero, thus the speed is kept at zero. Fig. 7b presents the dc-bus voltage and charging current. The voltage is controlled at 600V without a steady state error, and the charging current follows the shape of the voltage as the battery contains only a resistor and an ideal voltage source in the model.

B. V2G Mode of the Asymmetrical Six-Phase System

In this subsection configuration's capability of returning the energy back to the grid is demonstrated. Since a bidirectional dc-dc converter is not included in the simulation model, the battery is now represented with an ideal voltage source of E = 683V and a resistor of R_L=0.5Ω. Main test conditions are summarized in Table I.

Although this presents a different mode of operation the control is not altered, and the only difference is that now the reference for the dc-bus voltage has to be lower than the battery voltage, thus its reference is set to 680V. The higher dc-bus voltage is required due to the fact that the converter phase voltage has to have the first harmonic higher than the grid phase voltage due to a voltage drop on the machine windings, which can have high values primarily due to high stator resistance R_s of the machine (which is in this particular case 12.5Ω). Needless to say, for higher charging currents this voltage drop would increase linearly.

Fig. 8a presents the grid voltage and current. The current is in counter-phase with the voltage, which means that the energy is injected into the grid at the unity power factor. If compared to Fig. 4 for charging mode of operation, it can be seen that the grid current amplitude is slightly lower for V2G operation. This occurs regardless of the fact that the same voltage difference exists between the ideal voltage source of the battery and the dc-bus voltage, only in the opposite direction. The reason for this is that in the charging mode the grid has to produce the power that will charge the battery, as well as the power that will be transferred to heat. In contrast to this, in V2G mode the power transferred back to the grid is what is left from the battery discharging power after the power losses on the filter (i.e. machine). Thus, considering the fixed [v_g], grid current amplitude naturally reduces.

Fig. 8b shows the gird current spectrum, which has very small values of low order harmonics. Its THD is a bit higher than for the charging mode (Fig. 4b) because of the same ripple amplitude, which is determined by machine parameters and has a higher relative value (i.e. THD) for smaller funda-

TABLE I. TEST CONDITIONS

	Charging	V2G
E (V)	597	683
v_{dc} (V)	600	680
i_L (A)	6	-6
i_{dq} (A)	7.5	-6

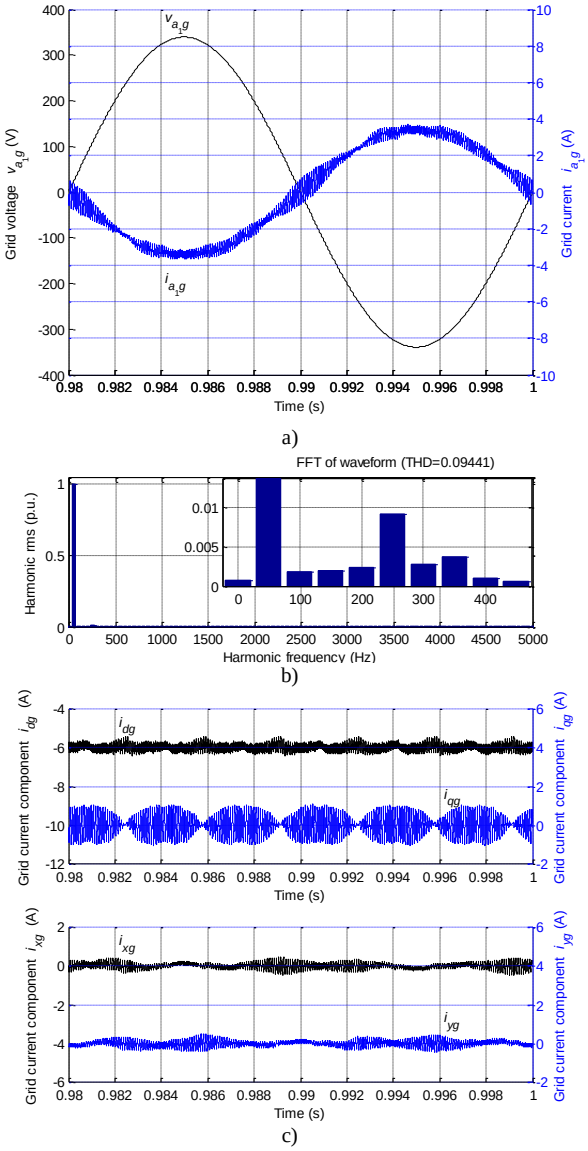

Fig. 8. V2G mode: (a) Grid phase voltage and current, (b) grid current spectrum, (c) grid current components.

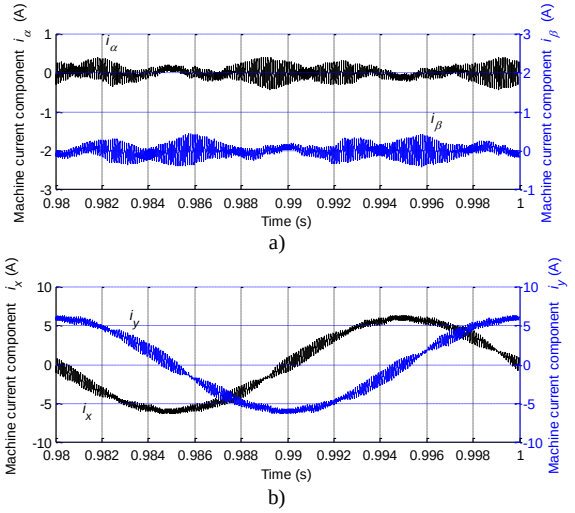

Fig. 9. Machine current componets: (a) i_α and i_β, (b) i_x and i_y.

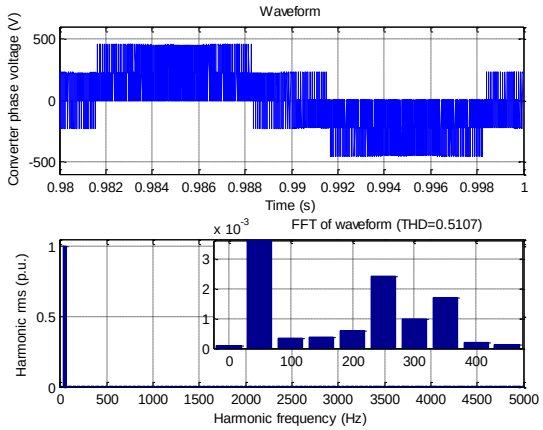

Fig. 10. Convereter phase voltage and spectrum.

mentals (as explained in the previous paragraph, grid currents are smaller for V2G mode). This current at the same time presents the machine's phase current. Grid current components are depicted in Fig. 8c. As in the charging mode, the *q*-, *x*-, and *y*-component are kept at zero, and the *d*-component has a non-zero value. However, it now has a different sign.

Fig. 9 shows machine's current components. The excitation is again transferred from the torque producing ($\alpha\beta$) plane to the non-torque producing (xy) plane. The xy components have a different sign compared to Fig. 5b.

Converter phase voltage and spectrum for V2G operation are given in Fig. 10. The spectrum shows only negligibly small values of low order harmonics.

Fig. 11a demonstrates that the torque has zero average value, and that the speed is kept at zero, so that the rotor does not have to be locked in this mode of operation either. Dc-bus voltage is controlled at 680V without a steady state error, as can be seen in Fig. 11b. The battery current has exactly the same value as in the charging mode, however it now flows in the opposite direction.

VI. Conclusion

The paper considers an integrated solution for EV battery charging using an asymmetrical six-phase machine. It thus proposes a new integrated on-board charging configuration that incorporates inverter and propulsion machine into the charging process. The main characteristics of the solution are that operation with zero average torque naturally results during the charging due to the specifics of the connection used, and that the charging operation requires opening of the machine's neutral points (hardware reconfiguration) and operation during charging and V2G modes in open-end winding configuration. Theoretical considerations are supported with simulation verification.

Acknowledgement

The authors would like to acknowledge the Engineering and Physical Sciences Research Council (EPSRC) for supporting the Vehicle Electrical Systems Integration (VESI) project (EP/I038543/1).

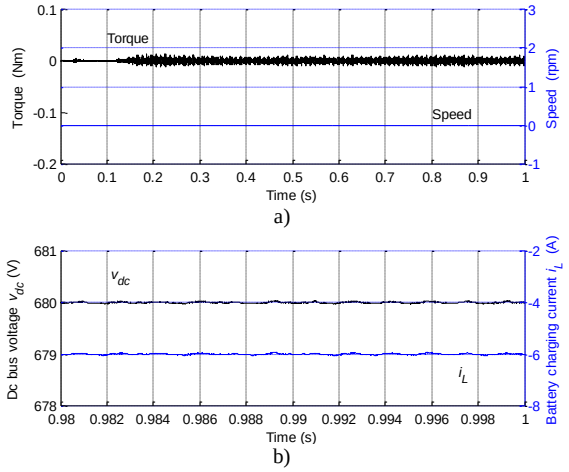

Fig. 11. (a) Machine torque and speed, (b) dc-bus voltage and charging current.

References

[1] ----------"Tesla Roadster specifications," http://www.teslamotors.com/display_data/teslaroadster_specsheet.pdf, 2009.

[2] J.M. Slicker, "Pulse width modulation inverter with battery charger," *US Patent* 4,491,768, 1985.

[3] S. Haghbin, S. Lundmark, M. Alakula, and O. Carlson, "Grid-connected integrated battery chargers in vehicle applications: review and new solution," *IEEE Trans. on Industrial Electronics*, vol. 60, no. 2, pp. 459-473, 2013.

[4] J. de Santiago, H. Bernhoff, B. Ekergård, S. Eriksson, S. Ferhatovic, R. Waters, and M. Leijon, "Electrical motor drivelines in commercial all-electric vehicles: A review," *IEEE Trans. on Vehicular Technology*, vol. 61, no. 2, pp. 475-484, 2012.

[5] S. Kinoshita, "Electric system of electric vehicle," *US Patent* No. 5,629,603, 1997.

[6] F. Lacressonniere and B. Cassoret, "Converter used as a battery charger and a motor speed controller in an industrial truck," *Proc. Eur. Conf. on Power Electr. and Applications EPE*, Dresden, Germany, CD-ROM, 2005.

[7] S. Haghbin, S. Lundmark, M. Alakula, and O. Carlson, "An isolated high-power integrated charger in electrified-vehicle applications," *IEEE Trans. on Vehicular Technology*, vol. 60, no. 9, pp. 4115-4126, 2011.

[8] L. De Sousa, B. Silvestre, and B. Bouchez, "A combined multiphase electric drive and fast battery charger for electric vehicles," *Proc. IEEE Vehicle Power and Propulsion Conference VPPC*, Lille, France, CD-ROM, 2010.

[9] I. Subotic, E. Levi, M. Jones, and D. Graovac. "On-board integrated battery chargers for electric vehicles using nine-phase machines," *IEEE Int. Electric Machines and Drives Conf. IEMDC*, Chicago, IL, pp. 239-246, 2013.

[10] E. Levi, R. Bojoi, F. Profumo, H.A. Toliyat, and S. Williamson, "Multiphase induction motor drives - a technology status review," *IET Electric Power Applications*, vol. 1, no. 4, pp. 489-516, 2007.

[11] E. Levi, M. Jones, S.N. Vukosavic, and H.A. Toliyat, "A novel concept of a multiphase, multimotor vector controlled drive system supplied from a single voltage source inverter," *IEEE Trans. on Power Electronics*, vol. 19, no. 2, pp. 320- 335, 2004.

[12] S. Haghbin, T. Thiringer, and O. Carlson, "An integrated split-phase dual-inverter permanent magnet motor drive and battery charger for grid-connected electric or hybrid vehicles," *Int. Conf. on Electrical Machines ICEM*, Marseille, France, pp. 1941-1947, 2012.

[13] M. Jasinski and M.P. Kazmierkowski, "Fundamentals of ac-dc-ac converters control and applications," in *The Industrial Electronics Handbook – Power Electronics and Motor Drives* (Chapter 16), edited by B.M. Willamowski and J.D. Irwin, CRC Press, 2011.

[14] E. Levi, "FOC: Field oriented control," in *The Industrial Electronics Handbook – Power Electronics and Motor Drives* (Chapter 24), edited by B.M. Willamowski and J.D. Irwin, CRC Press, 2011.